Modulation of brain and behavioural responses to cognitive visual stimuli with varying signal-to-noise ratios

Alberto Sorrentino [a,*], Lauri Parkkonen [b], Michele Piana [c], Anna Maria Massone [d], Livio Narici [e], Simone Carozzo [f], Massimo Riani [a], Walter G. Sannita [f,g]

[a] *CNR-INFM and Dipartimento di Fisica, Università di Genova, via Dodecaneso 33, 16146 Genova, Italy*
[b] *Brain Research Unit, Low Temperature Laboratory, Helsinki University of Technology, Espoo, Finland*
[c] *Dipartimento di Informatica, Università di Verona, Verona, Italy*
[d] *CNR-INFM, LAMIA, Genova, Italy*
[e] *Dipartimento di Fisica, Università "Tor Vergata", Roma, Italy*
[f] *Dipartimento di Scienze Motorie e Riabilitative, Università di Genova, Genova, Italy*
[g] *Department of Psychiatry, State University of New York, Stony Brook, NY, USA*

Accepted 23 January 2006

Abstract

Objective: To study behavioral and brain responses to variations in signal-to-noise ratio (SNR) of cognitive visual stimuli.
Methods: We presented meaningful words visually, embedded in varying amounts of dynamic noise, and utilized magnetoencephalography (MEG) to measure responses to the words. A multidipole model of the evoked fields was constructed to quantify the strengths and latencies of the neuronal sources at each noise level. The recognition rates of the words were measured in separate behavioral sessions.
Results: MEG revealed sequential activation of occipital and occipito-temporal areas (latencies 130–250 and 170–350 ms, respectively) followed by activity in superior temporal cortex (230–640 ms). The strengths and latencies of all identified sources followed functions similar to the SNR of the stimulus. The peak amplitudes and shortest latencies of all sources coincided with the maximum SNR of the stimulus. The occipito-temporal and temporal sources as well as the word recognition rate accurately followed the SNR of the stimulus whereas the early occipital source exhibited a more peaked dependence on the SNR.
Conclusions: Evoked responses expectedly peaked at the maximum SNR of the stimulus. Interestingly, early visual responses showed sharper peaks than longer-latency sources as a function of the noise level. This can be understood as the higher-level processes analyzing the stimuli more holistically and thus being less sensitive to the salience of simple visual features. The similar noise-dependence of the longer-latency sources and the recognition rate provides new evidence for the relevance of these activations in the recognition of written words.
Significance: This study contributes to the understanding of brain activity evoked by degraded stimuli with cognitive content.

1. Introduction

Degraded stimuli have been employed in psychophysics and neuroimaging studies to investigate sensory systems. Images of objects mixed with different levels or spatial distributions of random interference or reduced in their pixel intensity range (e.g. 'two-tone images') are often used in such studies of the visual system (Dolan et al., 1997; Pegna et al., 2004; Tanskanen et al., 2005; Tarkiainen et al., 1999). Analogously, auditory input can be masked by a varying amount of uncorrelated noise to alter the physical and perceptual qualities of the stimulus (Hari and Mäkelä, 1988; Muller-Gass et al., 2001). These studies typically utilize stimuli embedded in increasing amounts of noise so that the signal-to-noise ratio of the stimulus decreases monotonically.

---

* Corresponding author. Tel.: +39 034 9882 1450.
 E-mail address: sorrentino@fisica.unige.it (A. Sorrentino).

In contrast to the previous studies, we wanted to investigate brain responses to stimuli that not only change in terms of the amount of added noise but exhibit a unimodal peak, or resonance, in the signal-to-noise ratio. This approach has an interesting connection to the theory of stochastic resonance (Wiesenfeld and Moss, 1995), which explains the observed enhancement in the detectability of sub-threshold or otherwise weak signals in the presence of an optimal amount of random interference, usually referred to as 'noise'. Stochastic resonance is observed in both artificial and natural non-linear systems and is suggested to play a functional role in the central nervous system, where sources of intrinsic noise are ubiquitous. Several studies on visual perception employed experimental paradigms designed to meet the *threshold stochastic resonance* theory (Gingl et al., 1995), in which visual stimuli were embedded in random noise and subjected to an artificial gray-level threshold (Piana et al., 2000; Simonotto et al., 1997, 1999). In this study, however, we did not consider stochastic resonance as a model for the underlying brain processes or activity but only applied stimuli that are stochastically resonant.

To reach brain functions beyond primary sensory systems, we used words as a cognitive component in the stimulus. Magnetoencephalography (MEG) has shown that both visual and extravisual cortical areas are involved in the processing of letters and words presented visually (Helenius et al., 2002; Pylkkänen and Marantz, 2003; Raij et al., 2000; Salmelin et al., 1996; Xiang et al., 2001). Tarkiainen et al. (1999) noted that the addition of static Gaussian noise affects the responses to letters, symbols, and words, and were able to identify brain processes specific for letter strings.

The aim of this study was to characterize the brain responses—at multiple levels—to a cognitive visual stimulus that itself exhibits stochastic resonance. Magnetoencephalography (Hämäläinen et al., 1993) was used in this study to measure brain activity with temporal and spatial accuracy sufficient to reveal the cortical activation sequence. In addition, word recognition was tested behaviorally and compared with the estimated strengths of the neural sources at different levels of added noise.

2. Methods

2.1. Subjects

Nine healthy volunteers (3 females), with age ranging from 24 to 52 years (mean 36 ± 12 years), were recruited among university students and staff. Seven of the subjects were right-handed, one left-handed, and one ambidexterous. No subject had any history or evidence of systemic, neurological or ocular diseases. All had normal visual acuity with proper correction. Six of the subjects were native Italian speakers and three were Finnish. All subjects

gave their informed consent. The MEG recordings were approved by the Helsinki-Uusimaa Ethics committee.

2.2. Experimental paradigm

According to subject's native language, an Italian or Finnish word was randomly selected for each trial from a bank of 50 meaningful words, 4 letters each. The word was written with a monospaced Courier font at a constant gray level $w = 114$ (scale 0–255) and centred on a screen of 640×480 pixels with constant background intensity ($b = 128$). Noisy static images were obtained by adding to each pixel a random number uniformly chosen in $[-\eta, \eta]$ and thresholding the pixels on the letters at $t = 104$: pixels lighter than the threshold were unaffected while darker pixels were replaced by those of the noisy background. Dynamic noise was obtained by presenting static images in a rapid sequence. This procedure yielded degraded shapes of letters darker than the average background. We employed 5 levels of added noise, presented in separate blocks in a monotonically increasing series: $\eta = 12$, 16, 24, 40, 60 (see Fig. 1).

Dynamic noise was present continuously throughout each block to avoid noise-onset responses. In the sequence, each static image, whether noise + word or just noise, was shown for two frames at the rate of 60 frames/s. The duration of the embedded word stimulus was chosen as 8 images = 264 ms, which is sufficiently long so that the word is perceivable at the noise levels about the resonance and that its early offset response does not overlap temporally with the longer-latency onset responses. The word was followed by 22 images = 726 ms of noise so that the expected longest-latency responses decay before the next trial. Response averaging was trigged at the word onset; see Fig. 2.

The static images were created off-line and displayed as a sequence with the Presentation stimulus software package (Neurobehavioral System, Inc., Albany, CA, USA). The stimuli were delivered to the subject by a video projector and a back-projection screen inside the dimly lit magnetically shielded room. Stimuli were presented binocularly, with the viewing angle consistent with foveal vision.
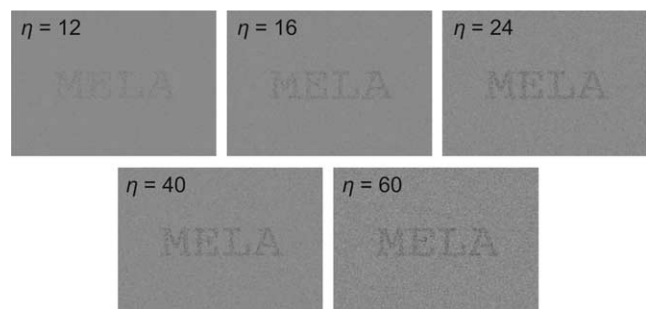

Fig. 1. Examples of the stimuli at the 5 noise levels. The visibility of the word is enhanced in these static images. MELA means 'apple' in Italian and 'paddle' in Finnish.
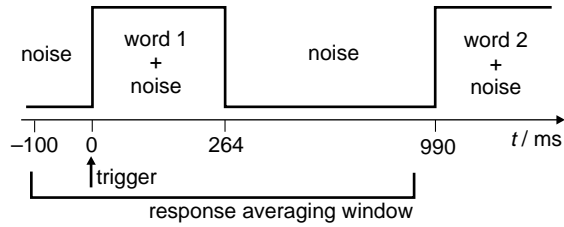
Fig. 2. Stimulus timing. Eight consecutive frames of the word+noise stimulus are followed by 22 frames of only noise at the same noise level.

Subjects were asked to fixate to a small cross in the center of the screen throughout the measurement.

The recognition of the words was tested by presenting all subjects with similar sequences of random words under the same conditions and in the same noise-level order as in the MEG experiment and asking them to read overtly the words they could. The speech output was recorded on a digital tape and analyzed off-line. These behavioral measurements were conducted after the MEG acquisition.

2.3. Stimulus properties

The mean contrast between the words and the background resulting from the thresholding procedure outlined above can be quantified. Let b be the background intensity level (gray level), w the intensity of the letters, and t the threshold. The intensity of a word pixel is thus

$$i = \begin{cases} w + r, & \text{if} \quad r + w < t, \\ b + r, & \text{if} \quad r + w \geq t, \end{cases} \quad (1)$$

where r is the realization of a random variable uniformly distributed over $[-\eta, \eta]$.

Eq. (1) suggests a probabilistic description of the stimulus. The probability density function (PDF) for a background pixel is

$$p_{\text{bg}}(\eta, i) = \begin{cases} \dfrac{1}{2\eta}, & b - \eta \leq i \leq b + \eta, \\ 0, & \text{otherwise}, \end{cases} \quad (2)$$

whereas the PDF for a pixel on a letter is:

$$p_{\text{w}}(\eta, i) = \begin{cases} \dfrac{1}{2\eta}, & w - \eta \leq i < t, \\ 0, & t \leq i < b + t - w, \\ \dfrac{1}{2\eta}, & b + t - w \leq i < b + \eta, \\ 0, & i \geq b + \eta. \end{cases} \quad (3)$$

Both PDFs are plotted in Fig. 3. For the dynamic stimulus, we can define a limiting *contrast-to-noise ratio*

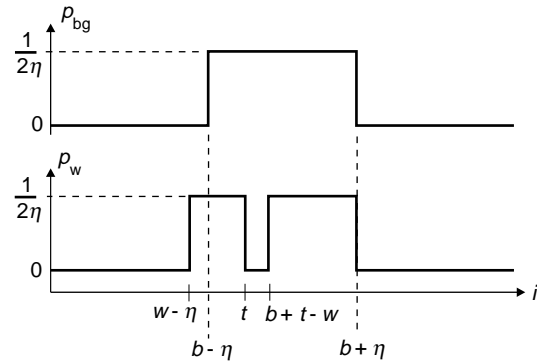$$\text{CNR}(\eta) = \frac{E\{p_{\text{bg}}(\eta)\} - E\{p_{\text{w}}(\eta)\}}{\eta} \quad (4)$$

Fig. 3. The background and letter pixel intensity distributions corresponding to Eqs. (2) and (3). The gap in the letter pixel intensity pdf is due to the thresholding procedure.

for the noise level η where $E\{p\}$ is the expectation value of the random variable p. The difference $E\{p_{\text{bg}}(\eta)\} - E\{p_{\text{w}}(\eta)\}$ represents the hypothetical mean contrast between the letters and the background. Substituting the probability density functions (2) and (3) yields:

$$\text{CNR}(\eta) = \begin{cases} \dfrac{1}{2\eta}\left[b - \dfrac{(w-b)(t-w) + \eta(w+b)}{2\eta}\right], & \text{if } \eta > w - t, \\ 0, & \text{otherwise}. \end{cases} \quad (5)$$

The limiting contrast-to-noise ratio is plotted in Fig. 4.

2.4. Data collection

The measurements were carried out in the Brain Research Unit of the Low Temperature Laboratory, Helsinki University of Technology, Espoo, Finland. MEG measurements were performed in a magnetically shielded room with a 306-channel MEG system (Elekta Neuromag Oy, Helsinki, Finland) consisting of 102 sensor units at distinct locations in a helmet-shaped array. Each sensor unit comprises 3 independent channels: one magnetometer and two orthogonal planar gradiometers. The planar
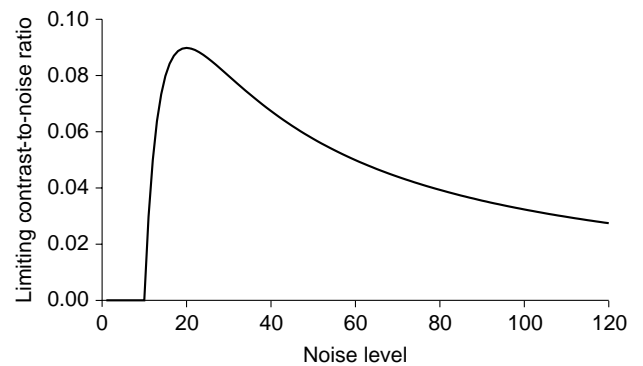

Fig. 4. Contrast-to-noise ratio of the stimulus as a function of the noise level as obtained from Eq. (4).

gradiometers give the maximum signal for the neural currents right beneath the sensor.

Environmental magnetic interference was suppressed by signal-space projection (SSP) (Parkkonen et al., 1999; Uusitalo and Ilmoniemi, 1997). The signal patterns corresponding to the highest eigenvalues of the correlation matrix of the raw signals from a measurement without a subject were identified; 3 of these patterns were projected out from the gradiometer data and 6 from the magnetometers.

MEG signals were filtered by a digital 6th-order Butterworth IIR filter (-3 dB at 172 Hz) and then sampled at 600 Hz. Eye blinks and horizontal and vertical eye movements were continuously monitored (electrooculogram, EOG) during the MEG measurement. Epochs with EOG or MEG exceeding 150 µV or 3 pT/cm, respectively, were excluded from further analysis. About 100 epochs free of artifacts were obtained for each noise level and averaged over time in windows of $[-100, 900]$ millisecond (time 0 at stimulus onset).

The MEG recording session lasted about 35 min, with approximately 5 min of rest between stimulus conditions.

Behavioral measurements were conducted separately but in the same conditions as the preceeding MEG recordings, i.e. the subjects seated in the MEG system and viewing the stimuli delivered in the same way as in the MEG sessions.

2.5. Anatomical MRIs and co-registration

Three anatomical landmarks (the nasion and the points anterior to the left and right ear canals) were utilized to establish a *head coordinate system*. The same landmarks were also identified in anatomical MRIs.

The position of the subject's head with respect to the MEG sensors was determined with the help of 4 marker coils placed on the scalp at known locations in the head coordinate system. The coils were localized prior to each experimental condition by briefly energizing them and measuring the resulting magnetic fields with the MEG sensors. During the data analysis, the estimated neural sources were always expressed in head coordinates thus the possible head movement across the conditions was compensated for.

Anatomical MR-images for all subjects were obtained using a General Electric Signa 3-T or a Siemens 1.5-T MRI scanner. The geometrical accuracy of the MR-image and the co-registration were verified by overlaying and visually comparing the MRI with the digitized head shape.

The MR-images of each subject were transformed to match the shape and sulcal/gyral structure of a standard atlas brain (Roland and Zilles, 1996) by a combination of an affine (Woods et al., 1998) and an elastic (Schormann et al., 1996) transformation. The obtained transformation was then applied to project the individual source locations onto the atlas brain for intersubject comparison.

2.6. Data analysis

The averaged MEG signals were low-pass filtered (zero phase shift FFT filter, corner frequency 40 Hz) and corrected for the baseline signal level in a window $[-100, 0]$ millisecond with respect to the stimulus onset.

The MEG signal sources were modeled with equivalent current dipoles (ECD), defined as the current dipoles best explaining the measured magnetic fields at a given time point. The ECD represents the synchronized activity in a small patch of the cortex (Hämäläinen et al., 1993). The location and orientation of an ECD are found with a non-linear search that minimizes the sum of the squared errors between the model and the measurements at each MEG channel. The fit was performed at time points when the averaged data exhibited a clear dipolar field pattern; a subset of the planar gradiometer channels centered about the dipolar pattern were used. At least 20 neighboring channels were selected for each fit. These single-dipole fits were then combined into a multidipole model in which only the dipole amplitudes were allowed to vary to best explain the signals on all MEG channels. Only dipole models accounting for more than 80% of the signal variance during the response peaks were accepted.

We employed a spherical conductor model—required for the estimation of the volume current distribution and the magnetic field due to it—as an approximation of the true shape of the intracranial volume. The sphere origin was determined from the anatomical MR-images of the subject. Since, responses were seen both in the occipital and temporal regions, we tested in two subjects whether two spheres fitted to the curvature of the intracranial volume at occipital and temporal regions would give different ECD locations. No significant differences were found, thus we modeled all the responses with a single sphere, fitted simultaneously to occipital and temporal regions.

The source model, consisting of multiple current dipoles, was constructed separately for each subject using data from the condition $\eta = 24$. This condition was chosen as it evoked the largest signals among all the conditions. The conformance of the model with data from the other conditions was verified by comparing the field maps and sources, and by monitoring the goodness-of-fit values. To further validate this approach of deriving the model from one particular condition, two additional checks were performed. First, in one subject, an alternative multidipole model was constructed based on a suboptimal noise level ($\eta = 12$). Compared to the original, this model gave essentially the same ECD positions, peak latencies and most importantly the source amplitudes as a function of the noise level. Second, areal RMS averages of the averaged MEG signals (6 pairs of planar gradiometer channels; no sensitivity to the source current orientation) above the identified source areas were examined for all the noise levels; the highest amplitudes were again obtained at the same noise level as
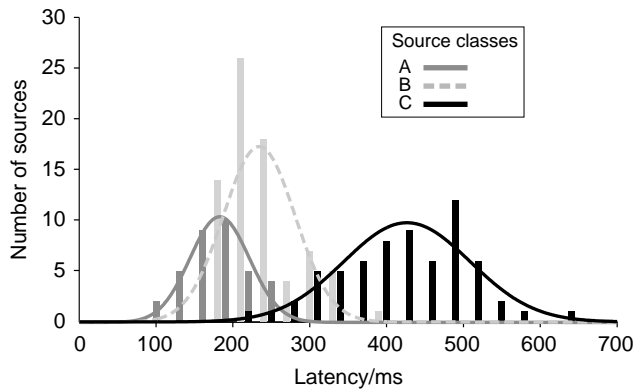
Fig. 5. Latency distributions of the 3 identified sources for all noise levels. The histograms represent the number of sources for all noise levels and all subjects at each latency interval. The parameters of the Gaussians modeling the distributions are obtained from the same data.

with the multidipole model and amplitudes decreased and latencies increased towards suboptimal noise levels.

The verified ECD model was then used to find the amplitudes of all the identified sources as a function of time across the averaging window; the locations and orientations of the dipoles were kept fixed and only the magnitudes were allowed vary to best fit the measured signals.

Due to notable intersubject variability (the peak dipole amplitudes range from 10 to 70 nAm at the resonant noise level) we normalized the source waveforms before averaging across subjects; the highest peak amplitudes and shortest latencies across all the noise levels of each source were scaled to unity.

3. Results

The ECDs of all subjects clustered in 3 classes by location and latency (Figs. 5 and 6). The ECD classes with shorter latency (hereafter referred to as A and B) were characterized by locations in medial occipital and occipito-temporal areas, respectively. Latencies from the stimulus onset varied 130–250 and 170–350 ms for A and B, respectively, with distributions partially overlapping.

The spatial resolution of MEG is not sufficient to clearly discern simultaneously active sources in the left and right primary visual areas, however, the medial occipital sources are most likely bilateral because of the full-field stimulus. The B sources were bilateral in 7 subjects and unilateral in 2 out of 9. A third source (class C) centered on the (superior) temporal areas, typically of both hemispheres (in 7 out of 9 subjects) was activated at latencies of 230–640 ms after stimulus onset, without significant temporal overlap with sources A and B. The dominant hemisphere of class C sources reflected the handedness of the subjects, i.e. right-handed subjects showed clear left-hemisphere dominance, in the left-handed subject the right hemisphere was dominant, and in the ambidexterous subject no clear lateralization was observable.

As a further verification of the separability of the three classes an analysis of variance (ANOVA) was performed for the peak latencies; the classes differ with $P < 0.05$.

The noise level affected the peak amplitudes and latencies of all sources. The average latency decreased and amplitude increased with increasing noise levels to reach the largest amplitude, shortest latency and smallest variance across subjects at the noise level 24. Latencies
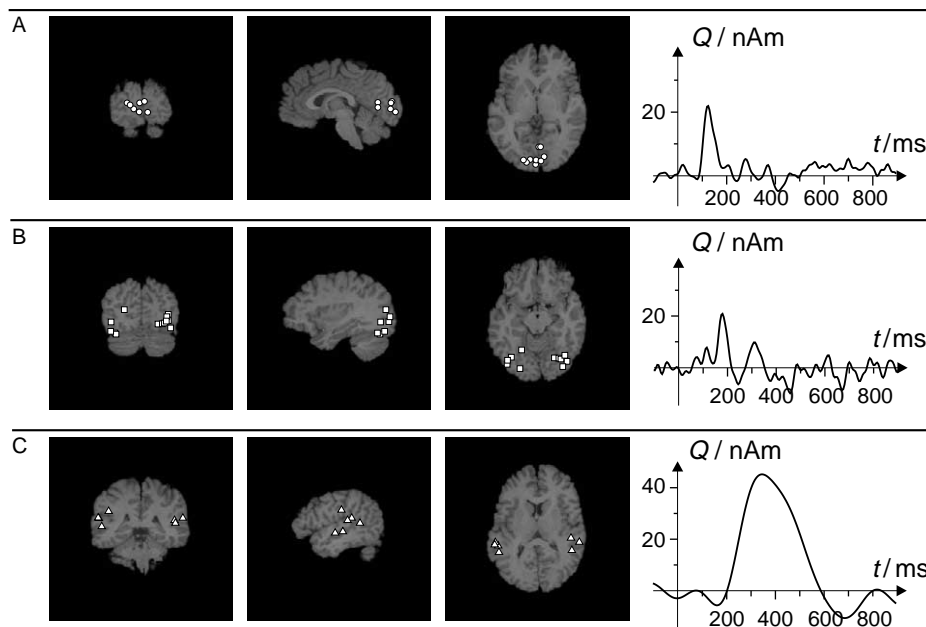

Fig. 6. Locations of the A, B and C sources of all subjects transformed onto the standard atlas brain, and the corresponding dipole amplitude waveforms of a single subject at the noise level $\eta = 24$.
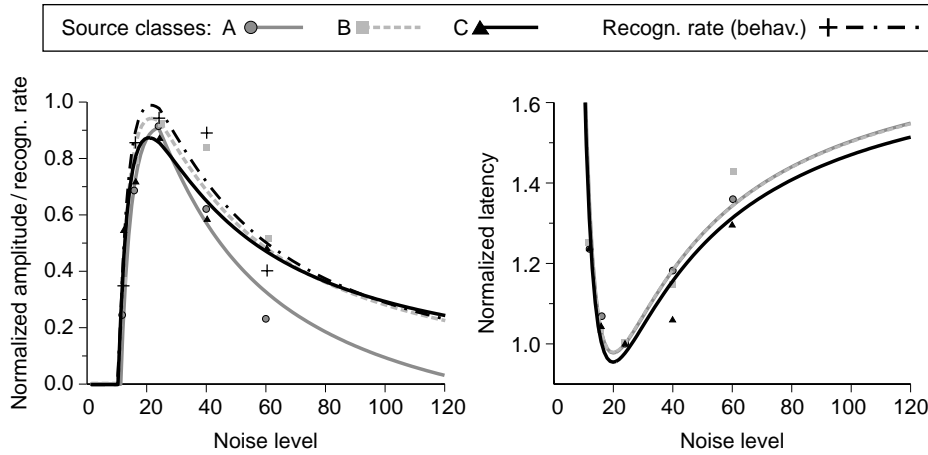
Fig. 7. The intersubject average of normalized source amplitudes, word recognition rates and source peak latencies as a function of the noise level (points). The contrast-to-noise ratio function is separately fitted to each data set (lines). The model function is inverted for the latencies.

thereafter increased at higher noise levels and the source amplitudes decreased.

The mean amplitudes and latencies of the 3 identified sources and the fitted functions derived from the mean contrast-to-noise ratio of the stimulus are shown in Fig. 7. A proper fit required a correction function $k(\eta, \beta)$ to be included in the numerator of the contrast-to-noise ratio (4) and a normalization factor α. The function $k(\eta, \beta)$ tunes the steepness of the model function at noise levels different than the resonant level $\eta = 24$.

The modified model function is thus:

$$\mathrm{CNR}(\eta) = \alpha \frac{E\{p_{\mathrm{bg}}(\eta)\} - k(\eta,\beta)E\{p_{\mathrm{w}}(\eta)\}}{\eta}. \tag{6}$$

We assume that $k(\eta, \beta)$ has a null effect at $\eta = 24 = b - t$ and increases linearly with the distance from this level:

$$k(\eta,\beta) = 1 + \beta|\eta - (b-t)|. \tag{7}$$

Substituting the probability density functions (2) and (3) yields:

$$\mathrm{CNR}(\eta) = \begin{cases} \frac{\alpha}{2\eta}\left[b - k(\eta,\beta)\frac{(w-b)(t-w) + \eta(w+b)}{2\eta}\right], & \text{if } \eta > w - t \\ 0, & \text{otherwise.} \end{cases} \tag{8}$$

Fig. 7 shows the amplitudes and latencies averaged across the subjects for each noise level and the fit of the contrast-to-noise function (8) to these averages. For the latencies, the fitted function was inverted and shifted along the y-axis. The CNR function was also fitted to the normalized behavioral data on the word recognition rate. The parameter values found in the fits are given in Table 1. The reduced χ^2 values computed for the three degrees of freedom are not far from 1, thus indicating an acceptable fit. For both amplitudes and latencies the fitted values of α were stable and expectedly around 10 (the maximum value of the model function is about 0.1, and the data were normalized to have a peak value of 1.0).

The β-parameters of source classes B and C and behavioral data do not significantly differ from zero ($P < 0.05$). In contrast, the β-value of source class A is significant with $P < 0.05$. This implies that the amplitude of class A sources can be modeled by means of (8) only with a substantial $k(\eta, \beta)$-correction, i.e. by considerably modifying the steepness of the model function.

4. Discussion

We employed degraded visual stimuli with words as cognitive content in a combined magnetoencephalographic

Table 1
Source classes and the behaviorally measured word recognition rate with the corresponding α and β parameters and χ^2 statistics for the amplitude and latency fits to the limiting contrast-to-noise function

Source	A	B	C	Recogn. rate
Location	Occipital	Occipito-temporal	Temporal	n.a.
α_{amp}	10.7	10.9	10.1	11.5
β_{amp}	4.9×10^{-4}	1.3×10^{-4} (n.s.)	5.0×10^{-5} (n.s.)	1.35×10^{-4} (n.s.)
χ^2_{amp}	2.57	2.68	1.95	2.27
α_{lat}	9.4	9.4	9.2	n.a.
β_{lat}	$< 10^{-7}$ (n.s.)	$< 10^{-7}$ (n.s.)	$< 10^{-7}$ (n.s.)	n.a.
χ^2_{lat}	1.79	0.59	1.91	n.a.

and behavioral experiment. These stimuli evoked magnetic responses at three distinct regions in the brain and at different latencies with respect to the presentation of the word.

The locations and temporal dynamics of the estimated neural sources allow some functional interpretation; the sites of sources A (occipital) and B (occipito-temporal) is congruent with that of striate and extrastriate visual cortices identified in humans by fMRI and PET techniques (Tootell et al., 1996). Moreover, class B is consistent, both in latency and location, with the previously identified letter-string specific source (Tarkiainen et al., 1999). The C class, located in (superior) temporal areas, was characterized by individual variability that may be more apparent than substantial. Although this source class could reflect general higher-level recognition processes, the observed temporal dynamics and locations are compatible with the known electrophysiological/neuromagnetic correlates of processing the semantics of language (the Wernicke–Geschwind model) (Hinojosa et al., 2001; Kober et al., 2001; Kuriki et al., 1998; Nobre et al., 1998; Poeppel and Hickok, 2004; Pulvermüller, 1999). Furthermore, the location is consistent with the previously reported sources of the magnetic counterpart of the N400 responses observed in concomitance to word comprehension (Helenius et al., 2002; Salmelin et al., 1996).

For all identified sources the amplitude maxima and latency minima (indicative, at large, of stronger neuronal activation and phase-locking to the sensory input (Hari, 1990)) and the smallest variance across subjects were reached at the middle noise level corresponding to the largest signal-to-noise ratio of the physical stimulus. More importantly, the source amplitudes and latencies as a function of the noise level were described with a good approximation by the contrast-to-noise function derived from the physical properties of the stimulus. The peak latencies of all sources tracked the contrast-to-noise function rather similarly, however, the amplitudes of the sources in striate visual areas (source class A) showed significantly more peaked dependence on the stimulus SNR than the other areas or the behaviorally measured word recognition rate. A recent MEG study by Hall et al. (2004) demonstrated that the contrast response functions of striate and an extra-striate visual area are different: the striate source can be characterized with a linear function while the extra-striate source saturates above a moderate contrast level. This is in a good agreement with our findings; the extra-striate source B reflects a process that is in the saturation regime within a wide window of noise levels about the maximum stimulus SNR and thus its dependence on the noise level is weaker than that of the striate source A with a linear contrast response function.

The temporal integration windows available for the processes underlying the evoked responses are also different. The early occipital source A with an average latency shorter than the duration of the stimulus reflects the transient onset of the stimulus and must thus rely on a short integration time while the longer-latency activity may take advantage of longer temporal windows. The source strengths behave consistently: the amplitudes of the longer-latency sources follow the limiting, i.e. infinite integration time, contrast-to-noise function of the stimulus more accurately than the early source A in the primary visual areas.

The difference between the A and other source classes can also be attributed to a more specific 'tuning' of the atomistic early visual processes to the simple physical features of the stimulus versus the more holistic longer-latency and higher-level processes analyzing the stimulus with larger receptive fields and thus being less sensitive to added uncorrelated noise. In addition, the higher-level recognition processes are likely to apply templates, acquired by learning, of letters and words, which renders them insensitive to a moderate degradation of sensory input. This is convincingly illustrated in a more general context by studies employing visual stimuli of objects sufficiently degraded to render them unrecognizable by a naive subject but easily identifiable once the non-degraded version has been presented to the subject (Dolan et al., 1997; Pegna et al., 2004).

Interestingly, the recognition rate of the words behaved similarly as the strengths of the occipito-temporal (B) and temporal (C) sources with respect to the noise level. This provides further evidence that the brain functions underlying these sources are likely to be essential for the recognition of visually presented words. The present results are also compatible with the assumption that there is no higher-tier word-recognition process; such activity would conceivably 'insensitize' the recognition rate further to the noise manipulation of the stimulus. Additional studies should, however, be conducted to address this point properly.

The consistency of the stimulus contrast-to-noise function with the 'threshold stochastic resonance' theory (Gingl et al., 1995) and its application in modeling the activation of involved cortical sources should be treated sensibly. Further research is needed to better understand the effects of visual 'noise' on brain processes and the possible interaction with intrinsic neuronal noise.

References

Dolan RJ, Fink GR, Rolls E, Booth M, Holmes A, Frackowiak RS, Friston KJ. How the brain learns to see objects and faces in an impoverished context. Nature 1997;389:596–9.

Gingl Z, Kiss LB, Moss F. Non-dynamical stochastic resonance: theory and experiments with white and arbitrarily coloured noise. Europhys Lett 1995;29:191–6.

Hall SD, Holliday IE, Hillebrand A, Furlong PL, Singh KD, Barnes GR. Distinct contrast response functions in striate and extra-striate regions of visual cortex revealed with magnetoencephalography (MEG). Clin Neurophysiol 2004;116:1716–22.

Hämäläinen M, Hari R, Ilmoniemi RJ, Knuutila J, Lounasmaa OV. Magnetoencephalography—theory, instrumentation, and applications to noninvasive studies of the working human brain. Rev Mod Phys 1993;65:413–97.

Hari R. The neuromagnetic method in the study of the human auditory cortex. Adv Audiol 1990;6:222–82.

Hari R, Mäkelä JP. Modification of neuromagnetic responses of the human auditory cortex by masking sounds. Exp Brain Res 1988;71(1):87–92.

Helenius P, Salmelin R, Service E, Connolly JF, Leinonen S, Lyytinen H. Cortical activation during spoken-word segmentation in nonreading-impaired and dyslexic adults. J Cogn Neurosci 2002;22(7):2936–44.

Hinojosa JA, Martin-Loeches M, Casado P, Munoz F, Fernandez-Frias C, Pozo MA. Studying semantics in the brain: the rapid stream stimulation paradigm. Brain Res Brain Res Protoc 2001;8(3):199–207.

Kober H, Moller M, Nimsky C, Vieth J, Fahlbusch R, Ganslandt O. New approach to localize speech relevant brain areas and hemispheric dominance using spatially filtered magnetoencephalography. Hum Brain Mapp 2001;14(4):236–50.

Kuriki S, Takeuchi F, Hirata Y. Neural processing of words in the human extrastriate visual cortex. Brain Res Cogn Brain Res 1998;6(3):193–203.

Muller-Gass A, Marcoux A, Logan J, Campbell KB. The intensity of masking noise affects the mismatch negativity to speech sounds in human subjects. Neurosci Lett 2001;299(3):197–200.

Nobre AC, Allison T, McCarthy G. Modulation of human extrastriate visual processing by selective attention to colours and words. Brain 1998;121(Pt. 7):1357–68.

Parkkonen LT, Simola JT, Tuoriniemi JT, Ahonen AI. An interference suppression system for multichannel magnetic field detector arrays. In: Yoshimoto T, Kotani M, Kuriki S, Karibe H, Nakasato N, editors. Recent advances in biomagnetism; proceedings of the 11th international conference on biomagnetism. Sendai: Tohoku University Press; 1999. p. 13–6.

Pegna AJ, Khateb A, Michel CM, Landis T. Visual recognition of faces, objects, and words using degraded stimuli: where and when it occurs. Hum Brain Map 2004;22:300–11.

Piana M, Canfora M, Riani M. Role of noise in image processing by the human perceptive system. Phys Rev E Stat Phys Plasmas Fluids Relat Interdiscip Topics 2000;62:1104–9.

Poeppel D, Hickok G. Towards a new functional anatomy of language. Cognition 2004;92(1–2):1–12.

Pulvermüller F. Words in the brain's language. Behav Brain Sci 1999;22(2):253–79 [see also discussion 280–336 review].

Pylkkänen L, Marantz A. Tracking the time course of word recognition with MEG. Trends Cogn Sci 2003;7(5):187–9.

Raij T, Uutela K, Hari R. Audiovisual integration of letters in the human brain. Neuron 2000;28(2):617–25.

Roland PE, Zilles K. The developing European computerized human brain database for all imaging modalities. Neuroimage 1996;4:39–47.

Salmelin R, Service E, Kiesilä P, Uutela K, Salonen O. Impaired visual word processing in dyslexia revealed with magnetoencephalography. Ann Neurol 1996;40(2):157–62.

Schormann T, Henn S, Zilles K. A new approach to fast elastic alignment with applications to human brains. Lect Notes Comp Sci 1996;1131:337–42.

Simonotto E, Riani M, Seife C, Roberts M, Twitty J, Moss F. Visual perception of stochastic resonance. Phys Rev Lett 1997;78:1186–9.

Simonotto E, Spano F, Riani M, Ferrari A, Levriero F, Pilot A, Renzetti P, Paodi RC, Sardanelli F, Vitali P, Twitty J, Chiou-Tan F, Moss F. fMRI studies of visual cortical activity during noise stimulation. Neurocomputing 1999;26–27:511–6.

Tanskanen T, Näsänen R, Montez T, Päällysaho J, Hari R. Face recognition and cortical responses show similar sensitivity to noise spatial frequency. Cereb Cortex 2005;15(5):526–34.

Tarkiainen A, Helenius P, Hansen PC, Cornelissen PL, Salmelin R. Dynamics of letter string perception in the human occipitotemporal cortex. Brain 1999;122(Pt. 11):2119–32.

Tootell RBH, Dale AM, Sereno MI, Malach R. New images from human visual cortex. Trends Neurosci 1996;19:481–9.

Uusitalo MA, Ilmoniemi RJ. Signal-space projection method for separating MEG or EEG into components. Med Biol Eng Comput 1997;35(2):135–40.

Wiesenfeld K, Moss F. Stochastic resonance and the benefits of noise: from ice ages to crayfish and SQUIDs. Nature 1995;373:33–6.

Woods RP, Grafton ST, Holmes CJ, Cherry SR, Mazziotta JC. Automated image registration: II. Intersubject validation of linear and nonlinear models. J Comput Assist Tomogr 1998;22(1):153–65.

Xiang J, Wilson D, Otsubo H, Ishii R, Chuang S. Neuromagnetic spectral distribution of implicit processing of words. NeuroReport 2001;12(18):3923–7.